Inhibitory Effect of Ammonium Tetrathiotungstate on Tyrosinase and Its Kinetic Mechanism

Kyung-Hee PARK,[a] Jae-Rin LEE,[a] Hwa-Sun HAHN,[a] Young-Hoon KIM,[a] Chang-Dae BAE,[a] Jun-Mo YANG,[b] Sangtaek OH,[c] Yu-Jin BAE,[d] Dong-Eun KIM,*[,d] and Myong-Joon HAHN*[,a]

[a] *Department of Molecular Cell Biology, Center for Molecular Medicine, Samsung Biomedical Research Institute, Sungkyunkwan University School of Medicine; Suwon 440–746, Korea:* [b] *Department of Dermatology, Sungkyunkwan University School of Medicine, Samsung Medical Center; Seoul 135–710, Korea:* [c] *PharmcoGenomics Research Center, Inje University; Busan 614–735, Korea: and* [d] *Department of Biotechnology and Bioengineering, and Department of Biomaterial Control, Dong-Eui University; Busan 614–714, Korea.* Received March 11, 2006; accepted June 15, 2006

Tyrosinase requires two copper ions at the active site, in order to oxidize phenols to catechols. In this study, the inhibitory effect of the copper-chelating compound, ammonium tetrathiotungstate (ATTT), on the tyrosinase activity was investigated. ATTT was determined to inactivate the activity of mushroom tyrosinase, in a dose-dependent manner. The kinetic substrate reaction revealed that ATTT functions as a kinetically competitive inhibitor *in vitro*, and that the enzyme–ATTT complex subsequently undergoes a reversible conformational change, resulting in the inactivation of tyrosinase. In human melanin-producing cells, ATTT evidenced a more profound tyrosinase-inhibitory effect than has been seen in the previously identified tyrosinase inhibitors, including kojic acid and hydroquinone. Our results may provide useful information for the development of whitening agent.

Key words tyrosinase; ammonium tetrathiotungstate; whitening agent

Tyrosinase (monophenol, *o*-diphenol : oxygen oxidoreductase, EC 1.14.18.1) is a binuclear copper enzyme, which is fairly ubiquitously distributed throughout organisms, and is known to play an important role in melanin synthesis.[1—4] Tyrosinase has been demonstrated to catalyze the hydroxylation of phenols to catechols, as well as the oxidation of catechols to quinones. The active site of tyrosinase consists of two copper ions, each coordinated by histidine residues within the active sites. These two coppers are known to be essential for the catalytic activities of this enzyme.[5] The binuclear copper active sites exist in all tyrosinases, regardless of source.[6,7] Therefore, the chelation of copper ions in this enzyme by flavonoid compounds or any other agents has been targeted as a strategy for the attenuation of tyrosinase activity, an objective relevant to cosmetic concerns, darkening problems in agricultural products, and certain medicinal reasons.[8—14]

Melanin pigments are synthesized by melanocytes, and are deposited throughout the epidermis. This process determines skin color.[15—18] Tyrosinase is involved in two different rate-limiting steps in melanin synthesis; namely, the hydroxylation of tyrosine to 3,4-dihyroxyphenylalanine (DOPA), and the oxidation of DOPA to dopaquinone.[19] The abnormal accumulation of melanin pigment can induce hyperpigmentations, such as freckles, melasma, and senile lentigines. These symptoms have responded, in the past, to treatment with depigmenting agents, including hydroquinone, ascorbic acid derivatives, retinoids, arbutin, and kojic acid. In particular, kojic acid (5-hydroxy-2-hydroxymethyl-4*H*-pyran-4-one) is a copper-chelator, which has been used as a cosmetic agent in skin-whitening formulations.[20] However, safer and more effective depigmenting agents are clearly needed, as kojic acid is not only carcinogenic, but its associated whitening effects are also somewhat weak.[21,22]

We have, in previous studies, applied several copper-specific chelating agents to mushroom tyrosinase, in an effort to screen an effective inhibitor, with the strategy of copper chelation at the active enzyme site.[23] Among these compound, ammonium tetrathiomolybdate (ATTM) has been shown to exert a significant inhibitory effect, as compared to the effect of other tested substances. In this study, we have attempted to characterize the effects of ammonium tetrathiotungstate (ATTT) on tyrosinase. ATTT has been identified as an effective decoppering reagent for copper storage-related diseases in both rats and sheep.[24,25] However, the kinetics of its inhibition in copper-containing enzymes has been the subject of only minimal exploration. Thus, we have attempted to evaluate the inhibition kinetics of tyrosinase by ATTT. Our kinetic studies revealed that ATTT was capable of the inactivation of tyrosinase *in vitro*. We have also verified the inhibitory effects of ATTT on tyrosinase in human melanocyte cells, as compared with those evidenced by other known inhibitors.

Experimental

Materials Mushroom tyrosinase, L-DOPA, kojic acid, and hydroquinone were purchased from Sigma. ATTT was obtained from the Aldrich Chemical Co.

Mushroom Tyrosinase Activity Assay The L-DOPA oxidation activity of mushroom tyrosinase was evaluated *via* measurements in the increase in absorbance at 492 nm, according to a method employed in a previous study.[9] In this evaluation, the reaction was initiated *via* the addition of the mushroom tyrosinase at a final concentration of 33.3 nM (4.0 μg/ml) to a 200 μl solution containing specified concentrations of L-DOPA and ATTT in 50 mM sodium phosphate buffer (pH 7.0). This reaction was conducted under a constant temperature of 25 °C, and the changes in absorbance were measured using a SPECTRA max PLUS spectrophotometer (Molecular Devices, Sunnyvale, CA, U.S.A.). The substrate-reaction progress curve was then analyzed by fitting to a single exponential followed by a linear phase (as shown below) in order to delineate the burst kinetics;

$$P(t)=Amp\cdot[1-\exp(-k_1\cdot t)]+k_2\cdot t \quad (1)$$

in which $P(t)$ is the product concentration at time t, Amp is the burst amplitude, k_1 is the rate constant of the burst phase, and k_2 is the rate constant of the linear phase.

Kinetic Analysis For the kinetic analysis, the complexing type of two-step inhibition pathway, which was derived from the method reported previously,[26—28] was applied, in which the following minimal mechanism was used (Scheme 1).

* To whom correspondence should be addressed. e-mail: mjhahn@yurim.skku.ac.kr; kimde@deu.ac.kr

$$E + \mathrm{ATTT} \underset{k_{\mathrm{off}}}{\overset{k_{\mathrm{on}}}{\rightleftarrows}} E\cdot\mathrm{ATTT} \underset{k_{-1}}{\overset{k_{+1}}{\rightleftarrows}} E^*$$

Scheme 1

E and $E\cdot$ATTT represent tyrosinase and the complex formed by the fast and reversible association of tyrosinase and ATTT, respectively. $E\cdot$ATTT has not yet been inactivated, but undergoes a slow conversion to form inactivated tyrosinase, E^*. k_{on} is the bimolecular association rate for the formation of $E\cdot$ATTT, and k_{off} is the dissociation rate of the $E\cdot$ATTT complex, whereas k_{+1} and k_{-1} represent the forward and backward rate constants of the inactivation step. The inactivation rate of tyrosinase at time, t, is given as:

$$\frac{d[E^*]}{dt} = k_{+1}[E\cdot\mathrm{ATTT}] - k_{-1}[E^*] = B[E_0] - A[E^*] \quad (2)$$

in which $[E_0]$ is the total enzyme concentration, and A and B, the apparent rate constants for the inactivation and reactivation, respectively, are expressed as follows;

$$A = \frac{k_{+1}[\mathrm{ATTT}]}{[\mathrm{ATTT}]+K_{\mathrm{I}}} + k_{-1}, \quad B = k_{-1} \quad (3)$$

The equilibrium binding constant for the inhibitor, K_{I}, equals $k_{\mathrm{off}}/k_{\mathrm{on}}$. The product formation can be written as follows:

$$[P]_t = \frac{k_{-1}v}{A}t + \frac{(A-k_{-1})v}{A^2}(1-e^{-At}) \quad (4)$$

in which $[P]_t$ is the product concentration formed after reaction time, t. v is the initial rate of reaction in the absence of the inhibitor.

Intrinsic Protein Fluorescence Measurement The fluorescence emission spectra were measured with a spectrofluorometer (JASCO FP-750) using 1 cm path-length cuvette. The enzyme (10 nM) was incubated at different ATTT concentrations at 25 °C for 30 min before the fluorescence measurement. For the tryptophan fluorescence measurement, an excitation wavelength of 280 nm was used, and the fluorescence emission was monitored at wavelengths between 300 and 420 nm.

Dilution of Inhibitor with Dialysis The mushroom tyrosinase (33.3 nM) was incubated for 1 h in 50 mM Tris–HCl buffer (pH 7.0), in either the absence or presence of 100 μM ATTT, at 4 °C. The enzyme solution was then dialyzed in the same buffer, in either the presence or absence of $CuSO_4$ (0.2 mM), $CuSO_4$ (1 mM), $CuCl_2$ (1 mM), $MgCl_2$ (1 mM), $MnCl_2$ (1 mM) or $ZnCl_2$ (1 mM), at 4 °C. The dialysis buffers were replenished every 2 h during the 6 h allowed for the entire reaction. After dialysis, the tyrosinase solution was removed, and the enzyme activity of L-DOPA oxidation was determined as described above. As a control, the mushroom tyrosinase, which had been incubated without ATTT, was also dialyzed and assayed under identical conditions.

Human Primary Melanocyte Culture and Lysate Preparation Human melanocytes were purchased from the Modern Tissue Technologies Inc. The cells were grown in 154 medium (Cascade Biologics) supplemented with HMGS (Cascade Biologics) and antibiotics (penicillin/streptomycin), in a humidified atmosphere containing 5% CO_2 in air at 37 °C. The cells were lysed with 0.05 M sodium phosphate at a pH of 7.0, 0.5% Triton X-100, and 0.1 mM PMSF. After sonication (20% amplitude for 1 min, Sonics and Material Inc.) and 10 min of centrifugation at 20000×g at 4 °C, the protein contents of the resulting supernatants were determined using a BCA kit, and the supernatant was employed in a tyrosinase activity assay, conducted in the presence of inhibitor.

Results and Discussion

Inhibitory Effect of ATTT on the Activity of Mushroom Tyrosinase Previously, we observed that the sulfur-conjugated molybdate compound proved an effective enzyme inhibitor.[23] As a result of this finding, in this study we tested another compound, ATTT, for its potential effects as an enzyme inhibitor, in which the tungstate ion is coordinated with sulfur rather than molybdate.

The time-course, in which the substrate was oxidized by tyrosinase in the presence of different ATTT concentrations, was recorded, as shown in Fig. 1. At each concentration of ATTT, burst kinetics of product formation was exhibited with increasing time until a straight line was apparent, which shows a steady state of enzyme reaction. The ATTT-mediated inhibition of the enzyme was found to occur in a concentration-dependent manner, as is shown in Fig. 1. As the concentration of ATTT increased, residual enzyme activity declined. However, it was never suppressed completely. The burst kinetic behavior of the enzyme activity in the presence of ATTT revealed that ATTT slowly but reversibly inactivated mushroom tyrosinase, with a fractional residual activity remaining after the achievement of a steady state. Thus, the observed inactivation kinetics suggests that copper ions at the active site of mushroom tyrosinase are chelated specifically by ATTT in a dose-dependent manner. Enzyme activity was almost abolished in the steady-state when the ATTT concentration reached 50 μM (Fig. 1).

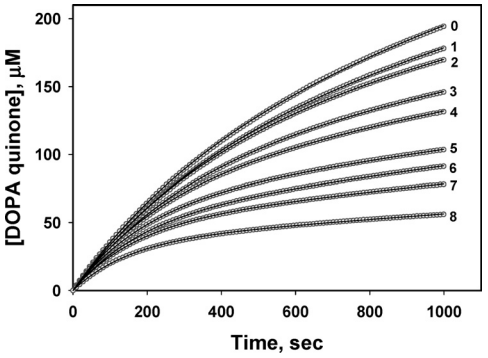

Fig. 1. Time-Courses for Inhibition of Mushroom Tyrosinase by ATTT

Shown is the inhibition kinetics of mushroom tyrosinase in the presence of various ATTT concentrations (circles). The ATTT concentrations for curves 0—8 were 0, 1.0, 2.0, 4.0, 6.25, 12.5, 18, 25, and 50 μM, respectively. The reaction mixture contained 8.0 mM L-DOPA and various concentrations of ATTT in the 50 mM sodium phosphate buffer, at a pH of 7.0. The final enzyme concentration was 4.0 μg/ml. The reaction was conducted at 25 °C, and the absorbance changes were measured at a 492 nm wavelength. Each of the kinetic time-courses was fit to the burst equation, and the fitting was overlaid onto the data (lines).

Inactivation Kinetics of ATTT on the Activity of Mushroom Tyrosinase In order to determine in detail the kinetic pathway by which ATTT effected the inactivation of mushroom tyrosinase, the time courses of the enzyme reaction observed at different ATTT concentrations were analyzed by fitting to the burst equation (Eq. 1). As is shown in Fig. 1, the kinetic data fit nicely with the burst equation. By equating Eq. 1 and Eq. 4, the apparent inactivation rate (A in Eq. 2 and Eq. 3) could be obtained using the fitting parameter of the burst equation (k_1 in Eq. 1). Thus, the fitting parameter (k_1) of the burst equation is used to establish the apparent forward inactivation rate constant at each of the inhibitor concentrations. The A values were plotted at increasing ATTT concentration points. The A values were found to be dependent on the ATTT concentrations, with a hyperbolic relationship (Fig. 2A). This indicates that the inhibitor binds reversibly to the enzyme, and subsequently inactivates the enzyme *via* a slow conformational change. An increase in [ATTT] resulted in both an increase in the inactivation rate (Fig. 2A) and a decrease in the residual activity, as can be seen by the slopes of the straight-line portions of the progress curves (Fig. 1), which falls under the rubric of slow-binding reversible inhibition kinetics.[26] The microscopic rate constant inherent to

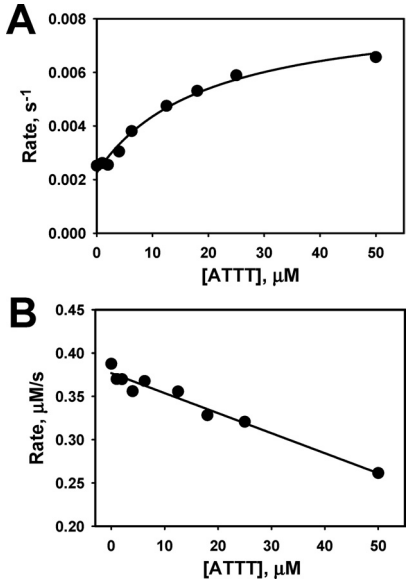

Fig. 2. Dependence of ATTT Concentration on the Apparent Forward Inactivation Rate Constants and the Initial Velocities

(A) Shows a hyperbolic increase in the apparent forward inactivation rate constants against increasing ATTT concentrations. The data were obtained from Fig. 1. The line indicates a hyperbolic fit with a y-intercept of 0.0023 s^{-1}. The fit provided an equilibrium dissociation constant (K_I) and an apparent forward rate constant of inactivation (k_{+1}) of 19.5 μM and 6.2×10^{-3} s^{-1}, respectively. (B) Shows the decrease in initial velocities with increasing concentrations of the inhibitor. The initial velocity was obtained from the slope of the burst phase at time zero, as shown in Fig. 1, which was calculated from the first derivative of the fitted burst equation. The data were then fitted to a linear line with a slope of 0.0023 s^{-1} and a y-intercept of 0.38 μM/s.

the reverse inactivation of the enzyme (k_{-1}) was measured as 2.3×10^{-3} s^{-1} *via* the extrapolation of the ATTT concentration to zero, which is the point of intersection at the ordinate of Fig. 2A. According to Eq. 3, the hyperbolic fit provided an equilibrium dissociation constant of $E\cdot$ATTT (K_I), and a forward rate inactivation constants (k_{+1}) of 19.5 μM and 6.2×10^{-3} s^{-1}, respectively.

Because the time-course of the ATTT-mediated inhibition of tyrosinase activity exhibited biphasic kinetics (Fig. 1), the inhibition of the enzyme by copper-chelating ATTT exhibited a pattern of reversible binding to the active site, subsequently induces a slow conformational change of the enzyme into an inactive state. Thus, the analysis of the initial slopes of the inhibition time-course during the early phase may provide a bimolecular rate of inhibitor binding to the enzyme, k_{on}. The first derivative of the burst equation with the fitting parameters acquired at time zero provided the initial early-phase slope, and initial slopes at different ATTT concentrations were plotted against [ATTT], as is shown in Fig. 2B. Increases in [ATTT] resulted in declines in the substrate-reaction rates during the early phases, characterized by a negative slope (Fig. 2B). The slope of the linear fit was 2.31×10^{-3} s^{-1}, reflecting the rate at which the inhibitor binds to the enzyme. The bimolecular rate of ATTT binding (k_{on}) was determined to be 6.9×10^{4} M^{-1} s^{-1} *via* the division of the slope with the enzyme concentration employed in the study (33.3 nM). Hence, the rate at which ATTT dissociates from the enzyme (k_{off}) was readily determined from the relationship of $K_I=k_{off}/k_{on}$, as 1.35 s^{-1}. The obtained kinetic parameters, which appear in Scheme 1, were listed in Table 1. In summary, ATTT binds slowly to the enzyme with a very small off-rate during the first steps of the kinetic pathway, a process which can be considered tight-binding. The enzyme–inhibitor complex subsequently undergoes conformational changes into the inactive form of tyrosinase, in which the copper ions at the active site are chelated by ATTT.

Table 1. Inhibition Constant and Microscopic Inactivation Rate Constants of the Mushroom Tyrosinase by ATTT

K_I (μM)	k_{on} (M^{-1} s^{-1})	k_{off} (s^{-1})	k_{+1} (s^{-1})	k_{-1} (s^{-1})
19.5±4.9	7.0 (±0.5)×10^4	1.35±0.3	6.2 (±0.6)×10^{-3}	2.3 (±0.1)×10^{-3}

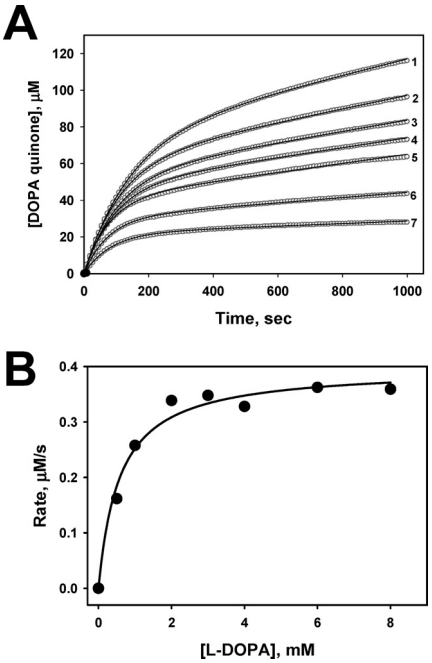

Fig. 3. Effects of Substrate Concentrations on ATTT Inhibition Kinetics

(A) Shown are the kinetic curves of the substrate reactions in the presence of different L-DOPA concentrations. L-DOPA concentrations for curves 1—7 were 0.5, 1.0, 2.0, 3.0, 4.0, 6.0 and 8.0 mM, respectively. Experimental conditions were identical to those referenced in Fig. 1, except that the ATTT concentration was fixed at 12.5 μM. Each of the kinetic time-courses was fit to the burst equation, and the fitting was overlaid onto the data (lines). (B) Shows the hyperbolic increase in initial velocities occurring in tandem with increasing L-DOPA concentrations. The initial velocity was obtained from the slope of the burst phase at time zero, as shown in (A), which was calculated from the first derivative of the fitted burst equation. The data were fitted to a hyperbolic equation with an amplitude of 0.40 μM s^{-1} and a $K_{1/2}$ of 0.58 mM.

Effects of Different L-DOPA Concentrations on the Inactivation Rate Constants by ATTT The kinetics of tyrosinase inactivation were investigated using different L-DOPA concentrations, in the presence of 12.5 μM ATTT (Fig. 3A). As was previously seen, substrate-reaction kinetics fit to the burst equation provided a series of apparent forward inactivation rates, designated as A. The initial slope of the burst phase at each substrate concentration was determined, and was plotted against the substrate (L-DOPA) concentration (Fig. 3B). The plots revealed a hyperbolic relationship between the substrate concentrations and the burst phase rates, indicating that increasing substrate concentrations slows the inactivation kinetics induced by ATTT. The hyperbolic fit was associated with an amplitude of 0.40 μM/s and a $K_{1/2}$ of 0.58 mM, reflecting the observed substrate binding rate and affinity in the presence of ATTT at a concentration of 12.5 μM, respectively. Thus, in the presence of 12.5 μM ATTT, L-DOPA (0.58 mM) binds to the enzyme at a rate of 1.04×10^{4} M^{-1} s^{-1} [0.2 μM s^{-1}/(0.58 mM·33.3 nM enzyme)].

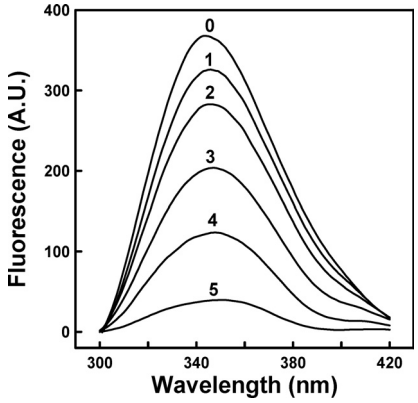

Fig. 4. Intrinsic Fluorescence Changes in the Presence of ATTT

Intrinsic fluorescence spectra were obtained after 30 min incubation of the enzyme (10 nM) with different concentrations of ATTT. The ATTT concentrations for curves 0—5 were 0, 3.1, 6.3, 12.5, 25, and 50 μM, respectively.

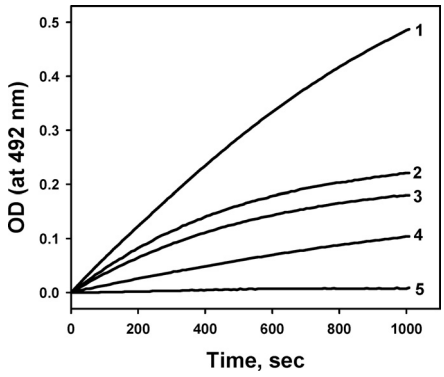

Fig. 5. The Effect of Dialysis on the Inhibitory Effect of ATTT on Mushroom Tyrosinase

The L-DOPA oxidation activity of the tyrosinase was measured as described in the text, and the increase in absorbance as the result of the oxidized L-DOPA was plotted. 1, Mushroom tyrosinase was dialyzed without ATTT treatment; 2, mushroom tyrosinase was incubated with ATTT and dialyzed in 50 mM Tris–HCl buffer (pH 7.4) with 1.0 mM $CuCl_2$; 3, mushroom tyrosinase was incubated with ATTT and dialyzed in 50 mM Tris–HCl buffer (pH 7.4) with 1.0 mM $CuSO_4$; 4, mushroom tyrosinase was incubated with ATTT and dialyzed in 50 mM Tris–HCl buffer (pH 7.4) with 0.2 mM $CuSO_4$; 5, mushroom tyrosinase was incubated with ATTT and dialyzed.

As compared to the observed binding rate of L-DOPA, $1.34\times10^5\,M^{-1}\,s^{-1}$, which was derived from the previously obtained k_{cat} and K_M values ($107.4\,s^{-1}$ and 0.8 mM, respectively),[29] the apparent binding rate of L-DOPA was reduced in the presence of ATTT. Hence, ATTT impedes the binding of the substrate to the enzyme as a competitive inhibitor, which is targeted against copper ions, and subsequently abolishes oxidase activity through the complexing of the copper ions. Under these conditions, the apparent inactivation is limited by the rate of the second step of the kinetic pathway (Scheme 1), namely, the unimolecular conversion of the $E\cdot$ATTT to E^*.

Dilution of ATTT with Copper Ions Partially Restores Enzyme Activity The kinetics inherent to the inhibition of tyrosinase by ATTT suggested that the inhibitor slowly binds and inactivates the enzyme *via* the chelation of the copper ions at the active site. Conformational change of the tyrosinase after ATTT binding was further investigated by the fluorescence emission spectra of inactivated tyrosinase. Changes in the fluorescence emission spectra of the tyrosinase (intrinsic protein fluorescence) after incubation with increasing concentrations of ATTT are shown in Fig. 4. Increasing ATTT concentration caused the fluorescence emission intensity to decrease without shift of emission maximum. These results showed that the conformation of ATTT-bound inactive tyrosinase is stable and different from that of uninhibited tyrosinase.

In order to characterize the reversibility of ATTT's tyrosinase-inhibitory activity, the enzyme which had been pre-incubated with ATTT was dialyzed against dilution buffer, in either the presence or absence of Cu^{2+}. As compared with the control experiment, in which the enzyme was pre-incubated with ATTT and dialyzed in the absence of copper ions, the enzyme dialyzed against dilution buffer in the presence of copper ions evidenced a partial recovery of oxidase activity by up to 70% (Fig. 5, Table 2). Interestingly, the reactivation of the enzyme appears to be dependent on the species of metal ions contained in the dilution buffer, as no restoration of enzyme activity was noted in conjunction with the presence of other metal ions, including magnesium, manganese, and zinc ions. These results indicate that ATTT does not participate in the irreversible formation of an enzyme–inhibitor complex at the enzyme active site, at which the copper ions

Table 2. Effect of Metal Ions on the Inhibitory Effect of ATTT on the Mushroom Tyrosinase

ATTT (100 μM)	Metal ions in dialysis buffer	Relative activity (%)[a]
−	—	100
+	—	0
+	0.2 mM $CuSO_4$	17.5±0.4
+	1.0 mM $CuSO_4$	54.1±0.2
+	1.0 mM $CuCl_2$	70.7±0.3
+	1.0 mM $MgCl_2$	0
+	1.0 mM $MnCl_2$	0
+	1.0 mM $ZnCl_2$	0

a) Relative activity was obtained from initial velocities of the kinetics shown in Fig. 4, which was calculated from the first derivative of the burst equation fitted to each time-course.

are reversibly chelated with ATTT. As a sufficient amount (100 μM) of ATTT had been pre-incubated with tyrosinase prior to the initiation of the dialysis reaction, the majority of the enzyme species were present in enzyme–ATTT complexed forms. Thus, copper–chelating ATTT may bind, slowly but reversibly, to the active site *via* competition with the substrates for copper ions. The enzyme–ATTT complex subsequently undergoes a reversible conformational change, ultimately leading to the inactivation of oxidase activity.

ATTT Has a Strong Hypopigmentory Effect on Melanoma Cells We then conducted a study to characterize the inhibitory effects of ATTT on the tyrosinase activity of melanocytes. The inhibitory effects of ATTT on melanogenesis in cultured melanocytes were tested and compared with other known inhibitors, including hydroquinone and kojic acid. ATTT, hydroquinone, and kojic acid evidenced dose-dependent inhibitory effect on the tyrosinase activity inherent to the cell lysates obtained from melanocytes (Fig. 6). ATTT exhibited significant inhibitory effects at concentrations between 5 and 100 μM. Tyrosinase activity was reduced more profoundly in the cells treated with ATTT than in the cells treated with hydroquinone or kojic acid. ATTT exhibited more profound inhibitory effects on the tyrosinase present in the melanocytes than did kojic acid, a well-known

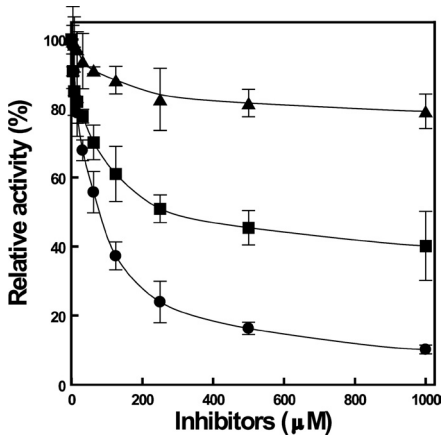

Fig. 6. Dose-Dependent Inhibitory Effects on Human Primary Melanocyte by ATTT, Kojic Acid, and Hydroquinone

Lysates of human primary melanocyte (20 μg/ml) were treated with increasing concentrations of inhibitors (3.9, 7.8, 15.6, 31.3, 62.5, 125, 250, 500, 1000 μM). The inhibitors shown are ATTT (circle), kojic acid (square), and hydroquinone (triangle). Effects on tyrosinase activity generated by these inhibitors are represented as relative activity (%, means)±S.E. from three independent tests.

whitening agent.[20,30] In conclusion, ATTT exerts an inhibitory effect on the activity of mushroom tyrosinase as well as on the tyrosinase in melanin-generating cells.

In this study, we have demonstrated the mechanisms underlying the inhibitory effects of ATTT on mushroom tyrosinase, and have determined that this copper–chelating reagent should prove useful in the cosmetic industry, as a whitening agent. The molybdenum analogue of ATTT, ATTM has been considered as a candidate for a therapeutic agent for Wilson's disease, as well as for its demonstrated efficacy as a whitening reagent.[31] Recent studies have extended its applicability, showing that it might also prove a useful anticancer and antiangiogenesis agent.[32] Although one study points to significant differences between ATTT and ATTM,[33] the similar structures and properties of these molecules, most notably their decoppering effects, suggest that ATTT might possess other properties in common with ATTM. Further study will be required in order to elucidate clearly all such possibilities.

Acknowledgments This work was supported by a grant (01-PJ3-PG6-01GN12-0001) from the 2001 Good Health R & D Project, Ministry of Health and Welfare, Republic of Korea and Brain Korea 21 Project in 2006.

References and Notes

1) del Marmol V., Beermann F., *FEBS Lett.*, **381**, 165—168 (1996).
2) Hearing V. J., Tsukamoto K., *FASEB J.*, **5**, 2902—2909 (1991).
3) Jimbow K., Park J. S., Kato F., Hirosaki K., Toyofuku K., Hua C., Yamashita T., *Pigment Cell Res.*, **13**, 222—229 (2000).
4) Sánchez-Ferrer Á., Rodríguez-López J. N., García-Cánovas F., García-Carmona F., *Biochim. Biophys. Acta*, **1247**, 1—11 (1995).
5) Solomon E. I., Sundaram U. M., Manchonkin T. E., *Chem. Rev.*, **96**, 2563—2605 (1996).
6) Cabanes J., García-Cánovas F., Lozano J. A., García-Carmona F., *Biochim. Biophys. Acta*, **923**, 187—195 (1987).
7) Robb D. A., "Copper Proteins and Copper Enzyme," CRC Press, Boca Raton, 1984, pp. 207—241.
8) Benathan M., Labidi F., *Acta Derm. Venereol.* (Stockh.), **77**, 281—284 (1997).
9) Chen Q. X., Kubo I., *J. Agric. Food Chem.*, **50**, 4108—4112 (2002).
10) Jones K., Hughes J., Hong M., Jia Q., Orndorff S., *Pigment Cell Res.*, **15**, 335—340 (2002).
11) Kubo I., Kinst-Hori I., *J. Agric. Food Chem.*, **47**, 4121—4125 (1999).
12) Qiu L., Zhang M., Sturm R. A., Gardiner B., Tonks I., Kay G., Parsons P. G., *J. Invest. Dermatol.*, **114**, 21—27 (2000).
13) Reish O., Townsend D., Berry S. A., Tsai M. Y., King R. A., *Am. J. Hum. Genet.*, **57**, 127—132 (1995).
14) Shimizu K., Kondo R., Sakai K., *Planta Med.*, **66**, 11—15 (2000).
15) Mills A. A., *Genes Dev.*, **15**, 1461—1467 (2001).
16) PerezBernal A., Munoz-Perez M. A., Camacho F., *Am. J. Clin. Dermatol.*, **1**, 261—268 (2000).
17) Sturm R. A., Box N. F., Ramsay M., *Bioessays*, **20**, 712—721 (1998).
18) Busca R., Ballotti R., *Pigment Cell Res.*, **13**, 60—69 (2000).
19) Hearing V. J., Jimenez M., *Pigment Cell Res.*, **2**, 75—85 (1989).
20) Cabanes J., Chazarra S., García-Carmona F., *J. Pharm. Pharmacol.*, **46**, 982—985 (1994).
21) Fujimoto N., Watanabe H., Nakatani T., Roy G., Ito A., *Food Chem. Toxicol.*, **36**, 697—703 (1998).
22) Takizawa T., Mitsumori K., Tamura T., Nasu M., Ueda M., Imai T., Hirose M., *Toxicol. Sci.*, **73**, 287—293 (2003).
23) Park K. H., Park Y. D., Lee J. R., Hahn H. S., Lee S. J., Bae C. D., Yang J. M., Kim D. E., Hahn M. J., *Biochim. Biophys. Acta*, **1726**, 115—120 (2005).
24) McQuaid A., Lamand M., Mason J., *J. Inorg. Biochem.*, **53**, 205—218 (1994).
25) Mason J., Mulryan G., Lamand M., LaFarge C., *J. Inorg. Biochem.*, **35**, 115—126 (1989).
26) Tsou C. L., *Adv. Enzymol. Relat. Areas Mol. Biol.*, **61**, 381—436 (1988).
27) Zhang R. Q., Chen Q. X., Xiao R., Xie L. P., Zeng X. G., Zhou H. M., *Biochim. Biophys. Acta*, **1545**, 6—12 (2001).
28) Park Y. D., Yang Y., Chen Q. X., Lin H. N., Liu Q., Zhou H. M., *Biochem. Cell Biol.*, **79**, 765—772 (2001).
29) Espin J. C., García-Ruiz P. A., Tudela J., García-Canovas F., *Biochem. J.*, **331**, 547—551 (1998).
30) Battaini G., Monzani E., Casella L., Santagostini L., Pagliarin R., *J. Biol. Inorg. Chem.*, **5**, 262—268 (2000).
31) Brewer G. J., Dick R. D., Johnson V., Wang Y., Yuzbasiyan-Gurkan V., Kluin K., Fink J. K., Aisen A., *Arch. Neurol.*, **51**, 545—554 (1994).
32) Pan Q., Kleer C. G., van Golen K. L., Irani J., Bottema K. M., Bias C., Carvalho M. D., Mesri E. A., Robins D. M., Dick R. D., Brewer G. J., Merajver S. D., *Cancer Res.*, **62**, 4854—4859 (2002).
33) Shah V. K., Ugalde R. A., Imperial J., Brill W. J., *J. Biol. Chem.*, **260**, 3891—3894 (1985).